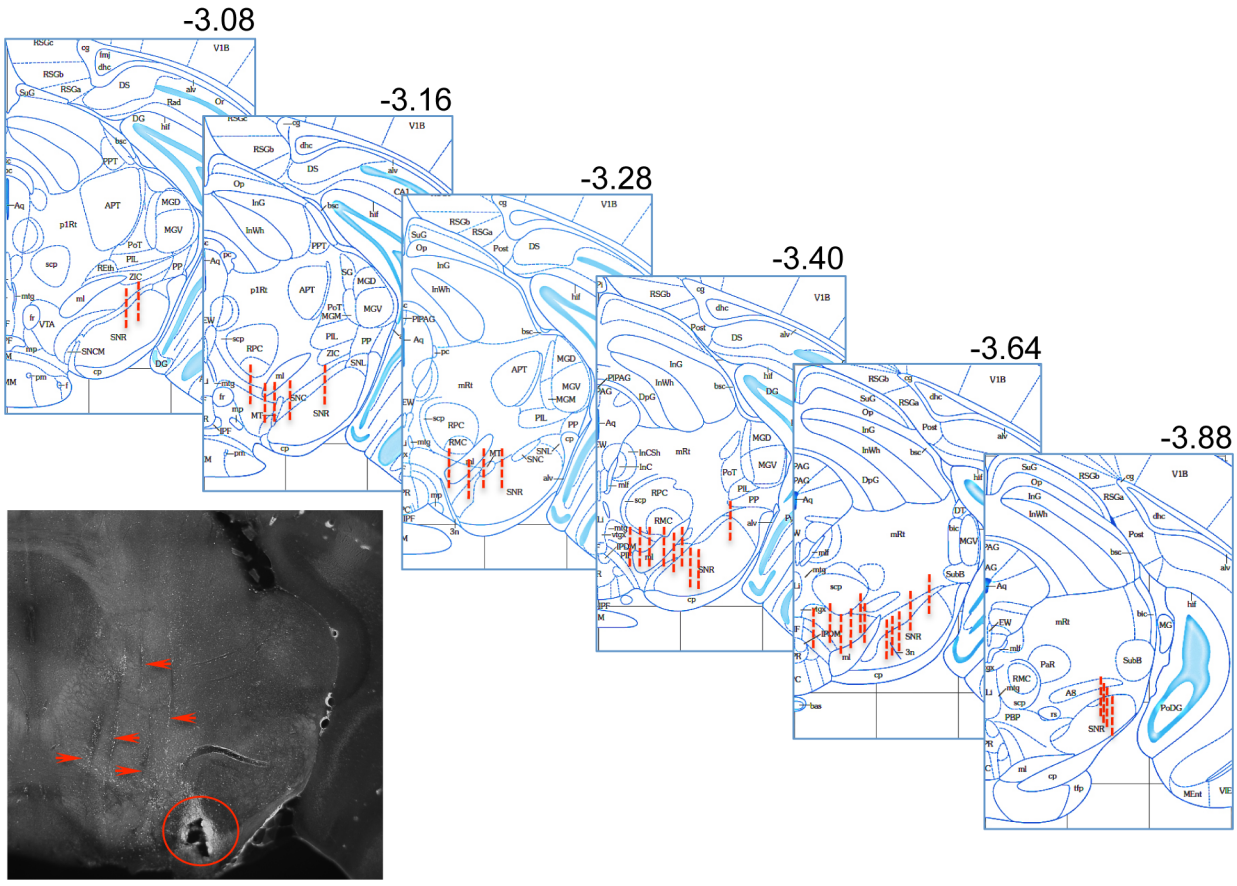

Supplementary Figure 1. *Midbrain recording sites*
Moveable arrays of 16 electrodes were implanted in five mice. Electrodes were advanced regularly between the recording sessions. The position of all recovered electrode tracks are indicated on the atlas sections. Numbers indicate position relative to bregma (mm). (inset) Image of a typical sample with tracks indicated by red arrow heads. Electrolytic lesions were made at the end of recording on a subset of wires (red circle). Briefly, electrode arrays were implanted near the position of the top of the red lines and lowered slowly into the SNc/VTA at the initatiation of recordings.

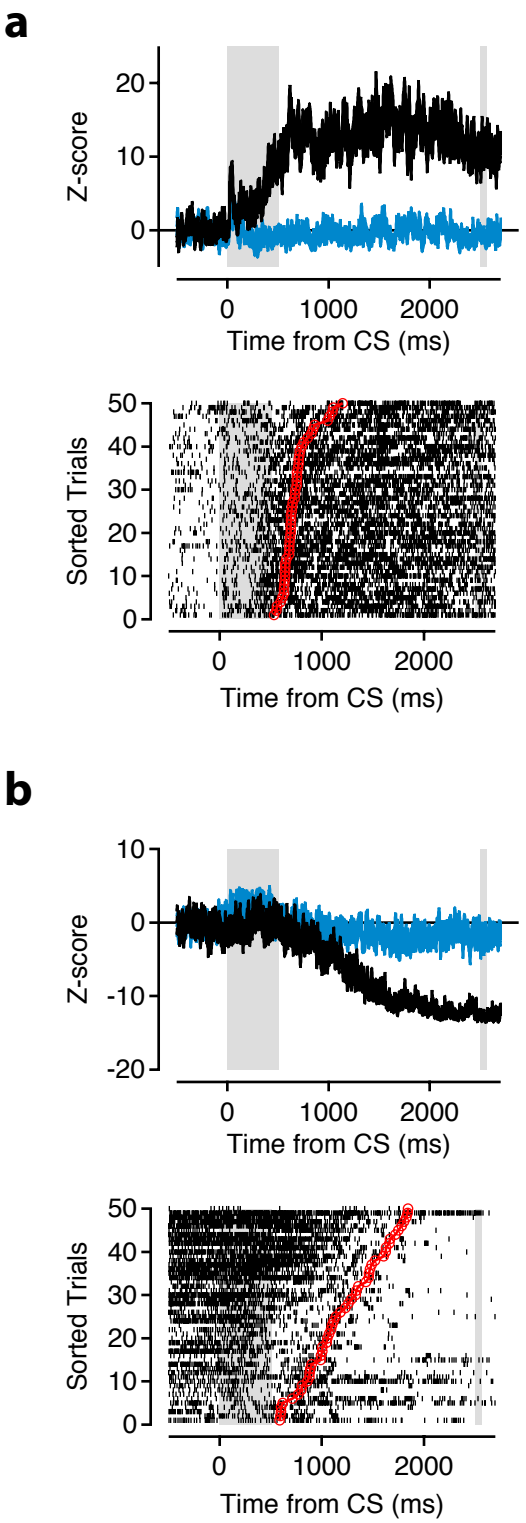

Supplementary Figure 2. ***Sustained responses during the trace period correlate with approach and consumption***
Example units showing sustained increasing (a) or decreasing (b) responses during the trace period. Upper panels show the PSTH as a function of time from the CS stimulus for acquisition (black) and extinction (cyan). Line thickness reflects the standard error. CS presentation and US delivery are indicated by gray shaded regions. Lower panels show raster plots for the same PSTHs sorted according to the latency to the first check of the reward port (red circles).

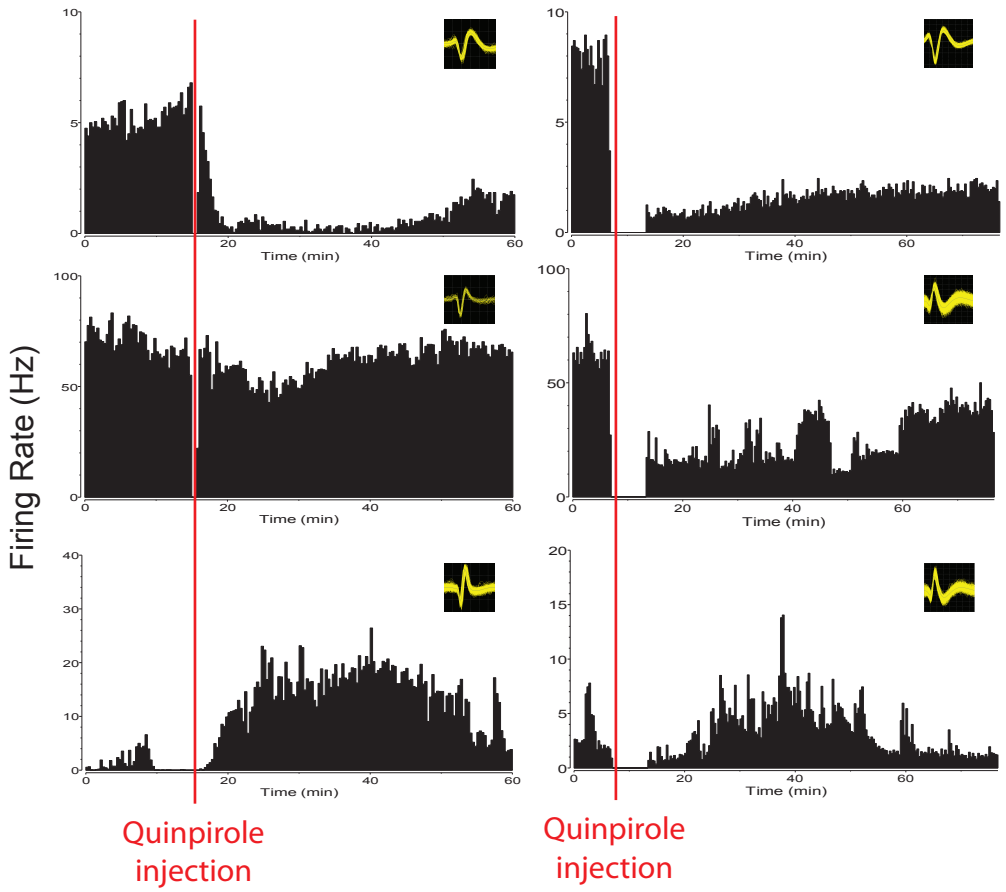

Supplementary Figure 3. Classes of unit chanes following quinpirole challenges
Firing rate as a function of time for 3 units recorded from the ventral midbrain in 2 mice (left and right columns) in response to quinpirole injection (red line). The top row are putative DA neurons identified based upon relatively broad waveforms and low baseline firing rates. Both exhibited classic conditioned responses of DA neurons and response latencies consistent with DA neurons. At all recording sites with identified DA units quinpirole injections produced suppressed firing. The bottom 2 rows are simultaneously recorded, non-DA units. Some units with decreases in firing in response to quinpirole challenge (middle) were not considered to be DA units due to the high baseline firing rates. Other units with low baseline firing rates, but narrow spikes often exhibited increases in baselne activity in response to quinpirole injection (lower panels).

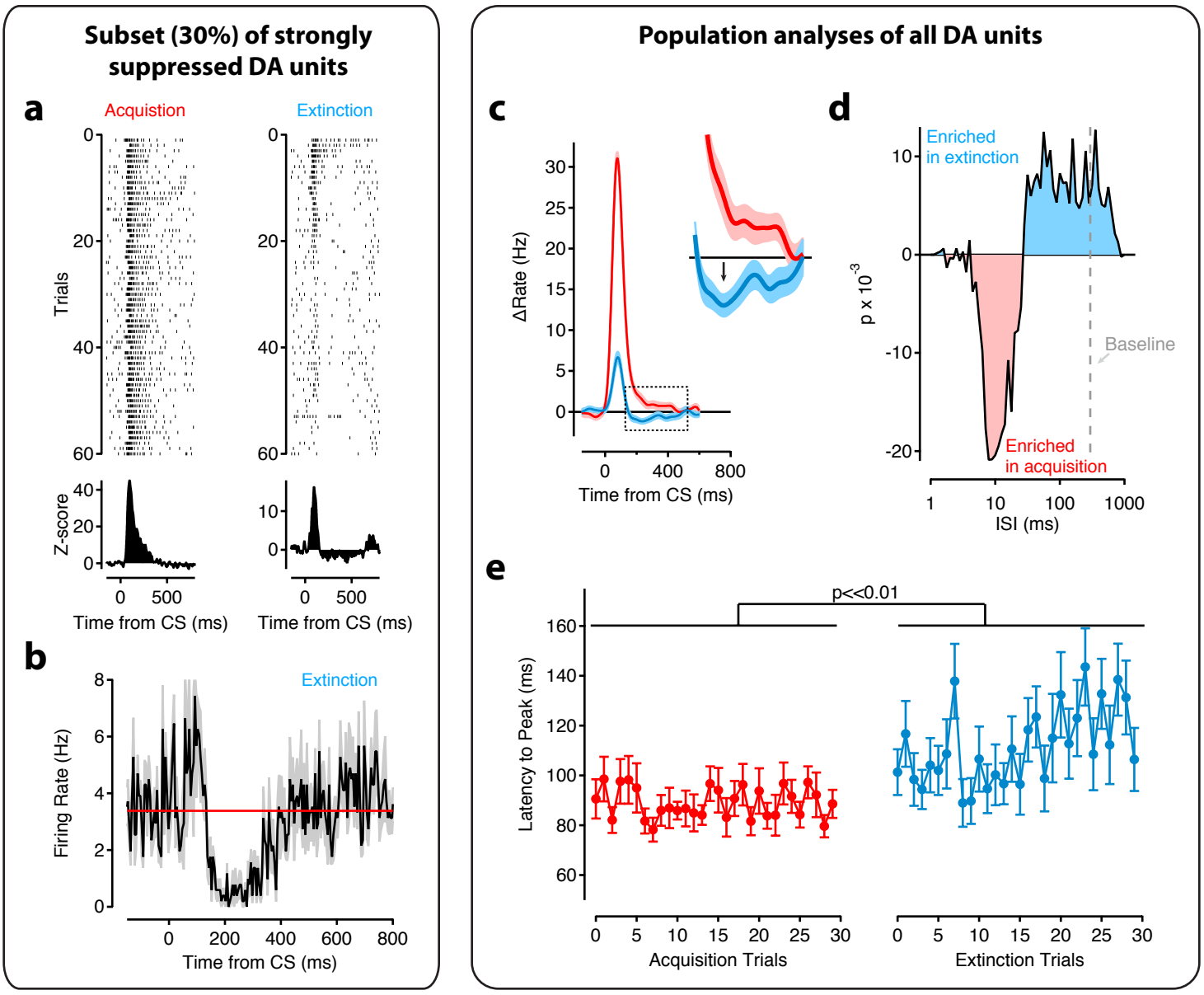

Supplementary Figure 4. ***Suppression of phasic activity of DA neurons during extinction***

A subset (~30%) of the DA neuron population showed clear and strong suppression with relatively little residual excitation late in extinction (a-b). (a) Example DA unit from Figure 2a replotted on an expanded timebase. (b) For this subset of DA units the mean response in extinction showed very clear suppression. Shaded area is standard error. (c-e) We also analyzed properties of the entire DA unit population for indirect evidence of enhanced inhibition in extinction. (c) We found that in the population average a suppression of firing below baseline was apparent after the excitatory phase. Population mean of the phasic response of DA units (baseline subtracted) for 40 trials of stable acquisition (red) and extinction (cyan). Boxed region indicates scaling of inset. Note the suppression of DA activity below baseline (<0) in extinction indicated by arrow. Shaded area indicates the standard error. The phasic excitation apparent in the population reflects differing timecourses of the decay of excitation often obscuring trials with a strong suppression of activity. To estimate the increase in suppression of activity across the population we calculated the difference in the intersike interval (ISI) histograms for acquisition and extinction around the time of the CS. Across the population extinction (cyan) produced an increase in the probability of long ISI events compared with those observed in acquisition (red). Suppression below baseline is revealed by an increase in the probability of observing ISI longer than predicted from basesline firing rate (indicated by gray line). We note that this increase is substantial given the bias that a burst of spikes produces both short ISIs and many ISIs, whereas a long suppression of firing produces a single ISI. (e) Finally, we considered whether there were changes in the phasic response of DA units even early in extinction when the phasic response persisted. We calculated the latency to the peak of the phasic response of DA units as a function of trials in acquisition (red, left) and extinction (cyan, right). Extinction produced a significant delay in the peak of the phasic DA response (ranksum test).

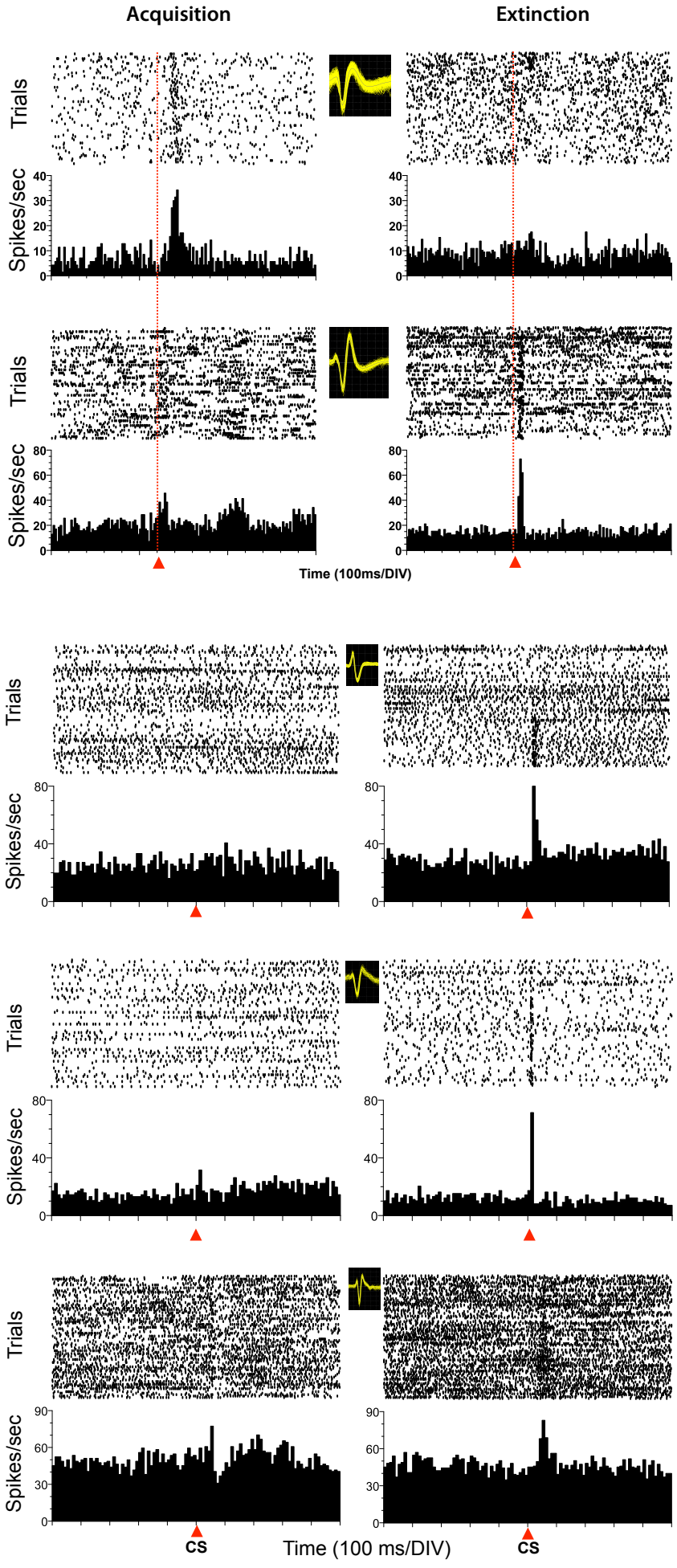

Supplementary Figure 5.
Diverse response patterns in extinction
For each graph the upper panel contains raster plots showing times of individual spike events across trials and aligned to the onset of the conditioned stimulus (CS) as indicated by the red arrowhead. Lower panel shows the peristimulus time histogram (PSTH) using 10 ms bins. The left column shows CS responses during blocks of acquisition (reward delivered following CS). Right column shows responses during extinction blocks (no reward delivered). Top two rows of units were a dopamine (upper) and GABA unit (lower) recorded simultaneously. Bottom 3 rows are "extinction cells" recorded in separate recording sessions.

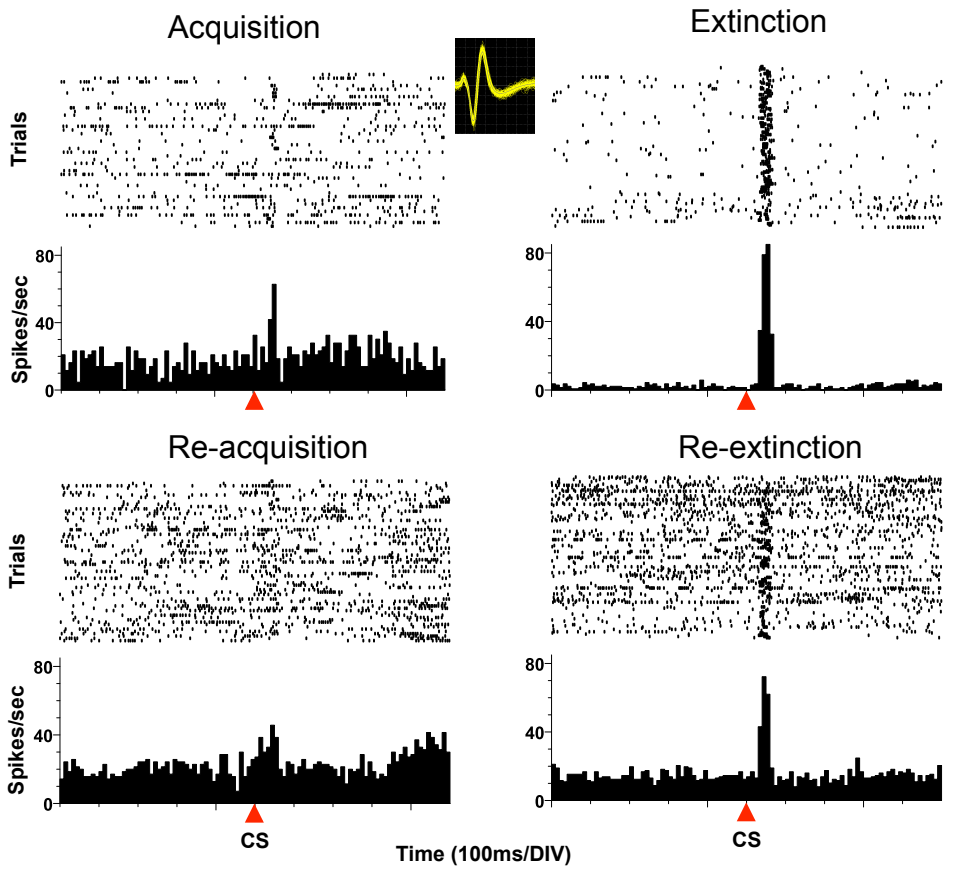

Supplementary Figure 6. ***Example cell response across multiple acquisition and extinction sessions***
For each graph the upper panel contains raster plots showing times of individual spike events across trials and aligned to the onset of the conditioned stimulus (CS) as indicated by the red arrow. Lower panel shows the peristimulus time histogram (PSTH) using 10 ms bins. The conditions of each block are indicated in text where Acquisition and Re-acquisition are blocks in which a water reward was delivered 2 seconds after CS onset and Extinction and Re-extinction are blocks in which the CS was delivered but no reward followed. Overlay of the waveforms for this cell is shown in inset.

a

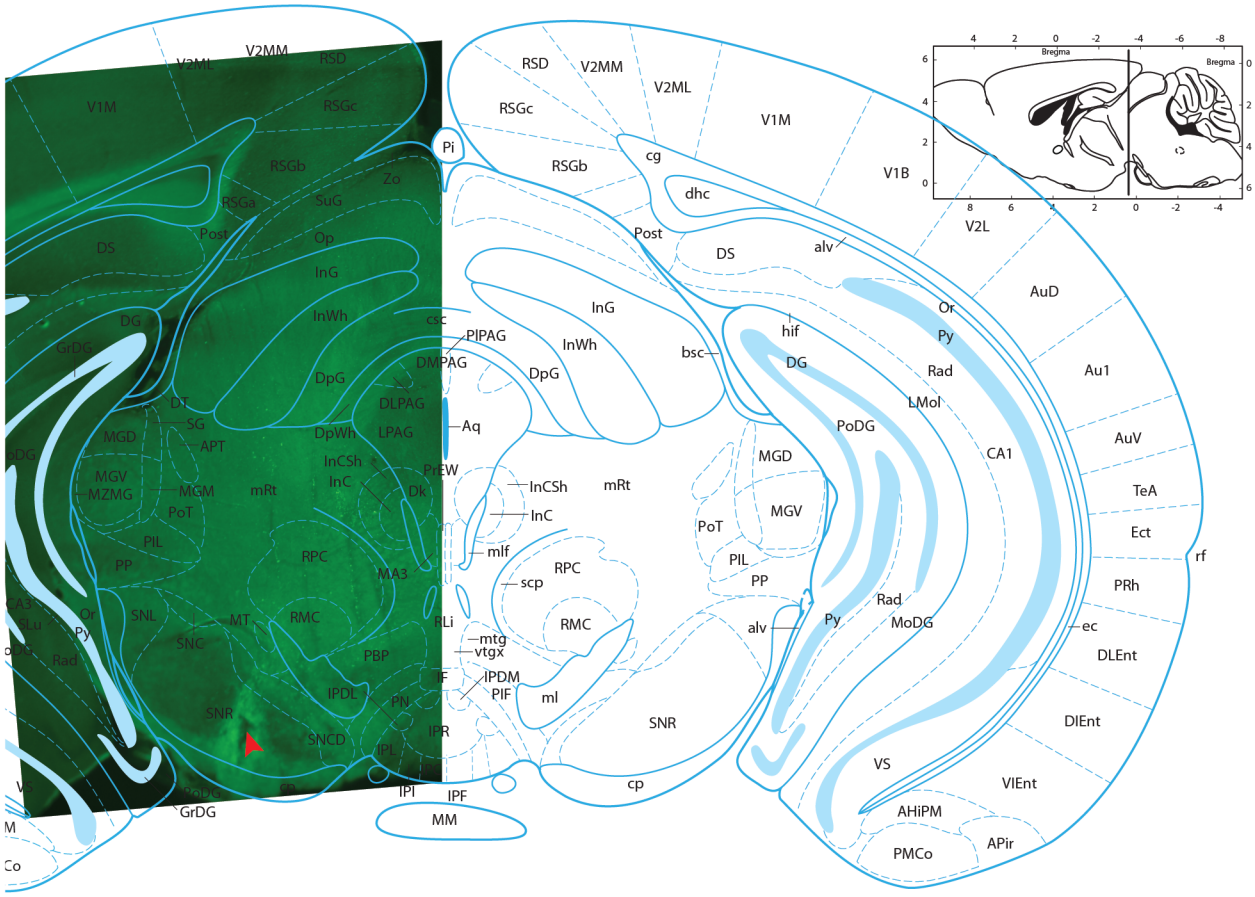

Bregma -3.40 mm

b

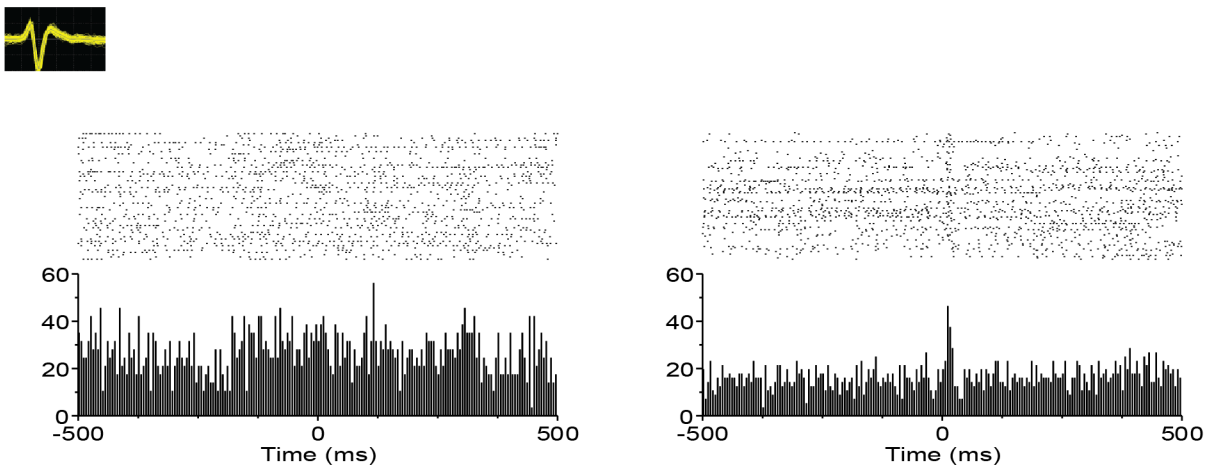

Supplementary Figure 7 ***Example recording electrode with extinction cells***

In some cases a lesion was made to mark electrode position at the end of recording on wires in which extinction cells were observed. An example histological section (a) and recorded unit (b) are shown. (a) The standard reference atlas is overlaid on the histological section obtained with the site of the electrode lesion marked by a red arrowhead. (b) An example 'extinction cell' unit recorded from the electrode shown in a.

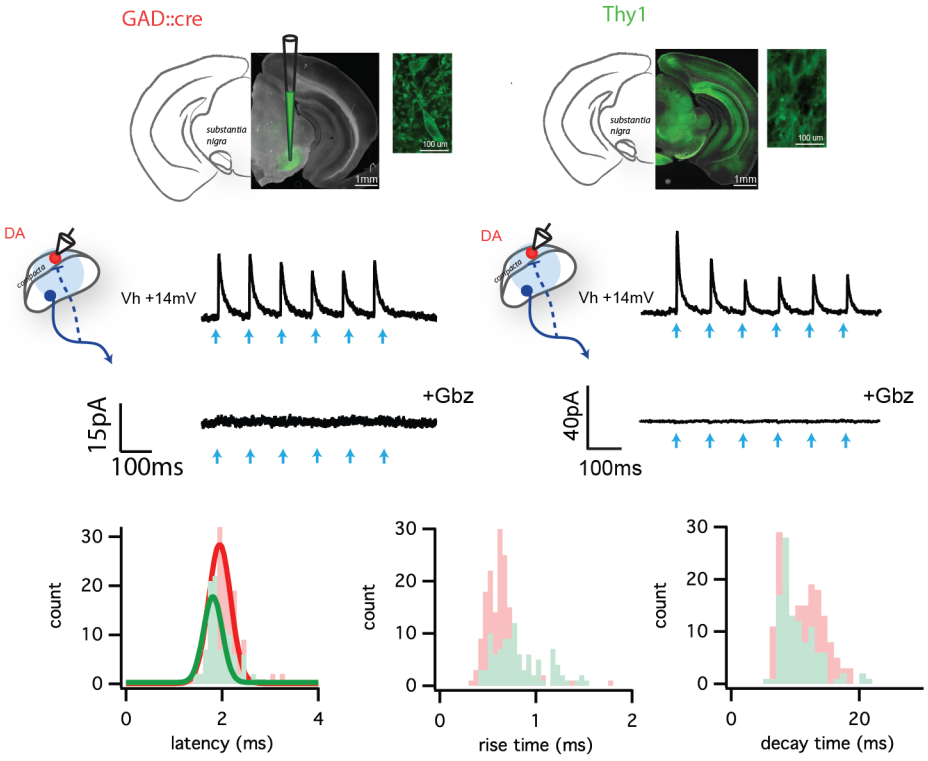

Supplementary Figure 8 *Evoked inhibition from SNr > DA projection*
Channelrhodopsin-2 (ChR2) expression was driven either by targeted injection of an adenoassociated virus in the substantia nigra pars reticulata (SNr; left) or by expression of a ChR2 transgene under control of the Thy1 promoter (right) that expressed in SNr GABAergic neurons but not dopaminergic (DA) neurons of the compacta (see Supp. Fig.s 8-10). Potsynaptic responses in DA neurons were recorded in voltage clamp with a holding potential (Vh) of +14 mV in the presence of blockers of excitatory transmission (AP5 & NBQX). Postsynaptic currents were insensitive to blockade of excitatory transmission, but were eliminated following application of gabazine (+Gbz; middle panels) in both cases. Individual light pulses (473 nm) are indicated by blue arrows. The latency, rise time and decay time (lower histograms) were not significantly different between vira-mediated expression (red) and transgenic expression (green) of ChR2.

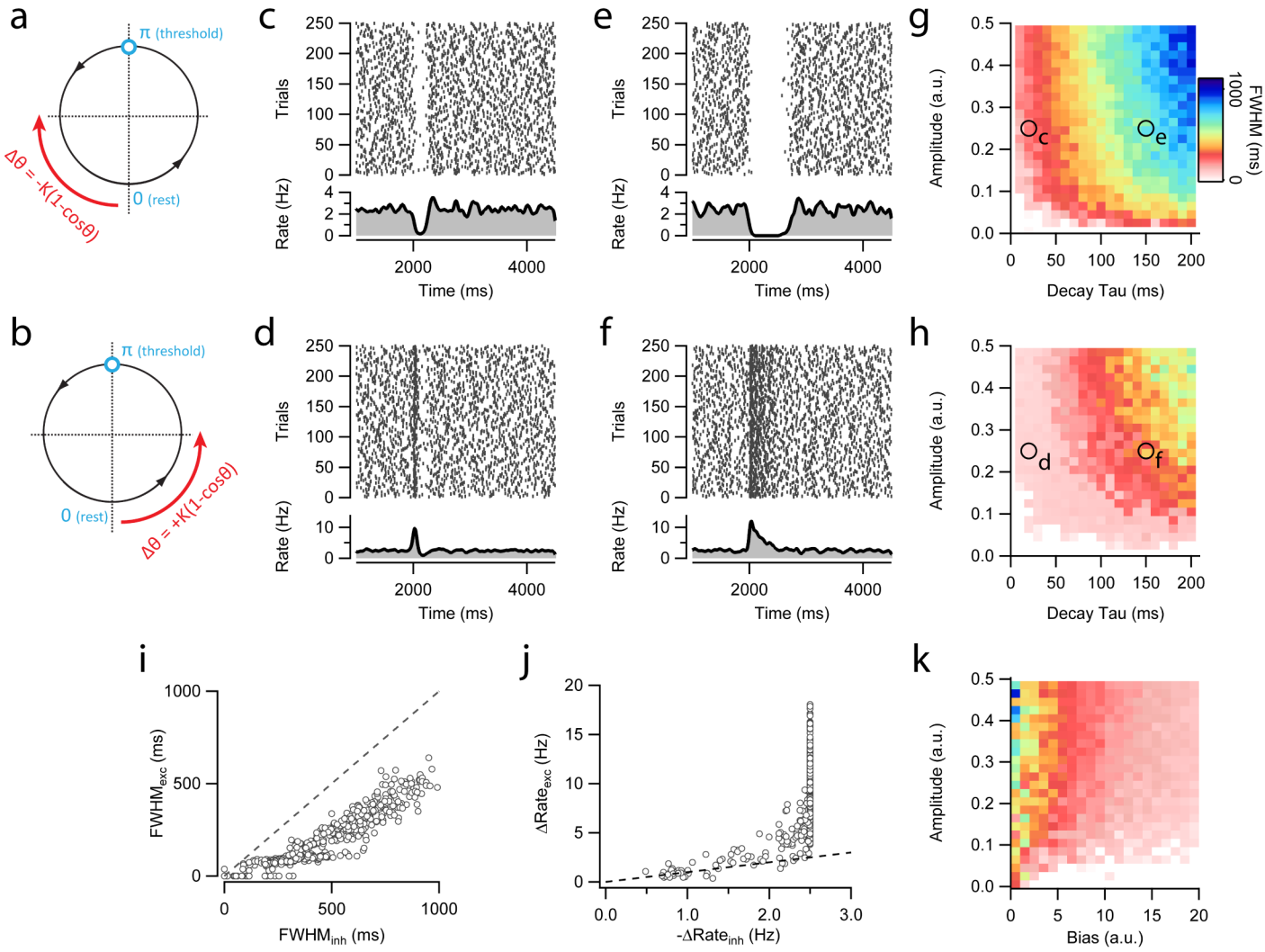

Supplementary Figure 9. ***Transient inhibition leads to sustained firing pauses in a dopamine neuron model***
(a-b) Schematic of the model perturbed by inhibition (a) or excitation (b). For a given oscillation frequency the response of the model to a variety of inhibition parameters (c,e,g) and excitation parameters (d,f,h) were tested. Example simulations for inhibition (c,e) and excitation (d,f) were selected from the parameter space as indicated in (g) and (h), respectively. (g-h) The full-width half maximum (FWHM) of suppression (g) or enhancement (h) of the peristimulus time histogram (PSTH) was calculated for each setting of amplitude and decay time constant of the monoexponential stimulus. (i) FWHM values for excitation and inhibition were plotted against each other for all tested parameters. Dashed line indicates the unity line. (j) Absolute values of the maximal change in rate for excitation and inhibition. The reduced FWHM in excitation is not a result of a reduced amplitude of modulation. (k) Resulting FWHM of inhibition for a range of amplitudes of inhibition and oscillation frequency (determined by a bias). FWHM strongly depends upon bias but it relatively independent of amplitude beyond a threshold amplitude of inhibition.

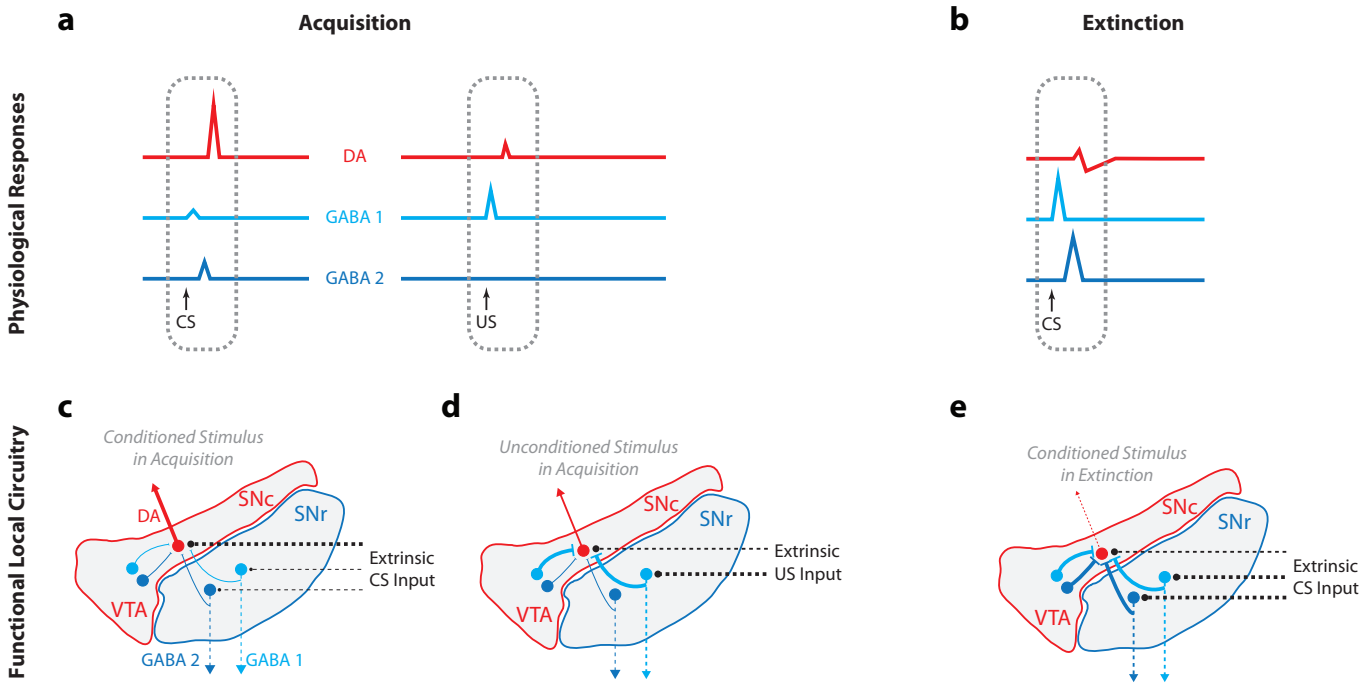

Supplementary Figure 10. Dynamic model of the midbrain inhibitory circuit during conditioning and extinction.
(a) Midbrain DA neurons receive both extrinsic inputs and local inhibitory inputs. With repeated pairing of a conditioned stimulus (CS) which predicts a reward (unconditioned stimulus [US]), the net local inhibition onto DA neurons at the time of the CS is reduced (either by a change in external drive to inhibitory neurons or plasticity of inhibitory neuron responses). The reduction of local inhibition (again either through changes in external drive or intrinsic plasticity) contributes to the emergence of a strong phasic activation of DA neurons to CS presentation. A schematic of the functional circuit diagram and the changes in firing rate are shown in the left and right columns, respectively. (c-d) The phasic response to the US of one population of local inhibition is, however, maintained in acquisition and contributes to the suppression of the DA response to a predicted US. As the schematic indicates (left) we propose that this inhibition is mediated by a presynaptic inhibitory mechanism due to the absence of a suppression of DA neurons below baseline in response to a predicted US. (c) A CS presented in the absence of a US (extinction) gradually enhances the phasic responses of both populations of midbrain GABA neurons contributing to the suppression of the phasic response of DA neurons to the CS_{ext}. A combination of presynaptic and postsynaptic inhibition at two distinct latencies is proposed to lead to the biphasic patterns of DA phasic responses observed in extinction (e).